22

Assessing Growth and Response to Therapy in Murine Tumor Models

C. Patrick Reynolds, Bee-Chun Sun, Yves A. DeClerck, and Rex A. Moats

Summary

Rodent models provide an important means of assessing antitumor activity vs toxicity for new cancer therapies. Tumors are often grown subcutaneously on the flank or back of animals, allowing accurate serial determination of tumor volume with calipers by measuring the tumors in three dimensions. The advantages of assessing tumor volume in subcutaneous tumors must be balanced against the potential artifacts induced by growth of tumor cells in subcutaneous tissue. Various orthotopic models have been developed. However, they are more labor-intensive and generally do not allow accurate assessment of tumor growth and/or response unless investigators have access to small animal cross-sectional imaging. Use of small-animal magnetic resonance imaging (MRI) allows one to assess the growth and response of intracavitary tumors, but the cost and labor-intensive nature of MRI limits its use in drug testing. Another approach to intracavitary solid tumor models is the intravenous injection of tumor cells, which can produce lung, liver, or bone metastases (depending on the cell line used), whereas direct injection of tumor cells into the femur or tibia of mice can cause local growth in bone. Progression of both lung metastases and bone lesions can be assessed by small-animal analog X-ray techniques that are more easily available and less labor-intensive to use, and are proving useful for selected therapeutic and biological studies.

Key Words

Mouse xenograft; tumor volume; bone metastases; chemotherapy; radiograph.

1. Introduction

Rodent models provide an important means of assessing antitumor activity vs toxicity for new antineoplastic drugs, and they provide a key component of preclinical developmental therapeutics for cancer. Syngeneic rat and mouse tumors played an important role in early cancer drug development ***(1–3)***, but these have largely been surpassed by the use of xenografted human solid

From: *Methods in Molecular Medicine, vol. 111: Chemosensitivity: Vol. 2: In Vivo Models, Imaging, and Molecular Regulators*
Edited by: R. D. Blumenthal © Humana Press Inc., Totowa, NJ

tumors in athymic (*nu/nu*) mice, in severe combined immunodeficiency (SCID) mice, or in athymic rats ***(4–8)***. Human leukemia cells injected intravenously into nod/SCID mice can provide a model of acute lymphoblastic leukemia that is being used for preclinical therapeutic studies ***(9–11)***. Although the limitations of rodent models in predicting clinically active agents are well recognized, they still provide an important component of preclinical testing, and significant responses in multiple xenograft models increase the possibility of a new drug having clinical activity ***(12)***.

Solid tumors are often grown subcutaneously on the flank or back of animals to allow an accurate serial determination of tumor volume with calipers by measuring the tumors in three dimensions ***(13)***. The advantages of assessing tumor volume in subcutaneous tumors must be balanced against the potential artifacts induced by growth of tumor cells in subcutaneous tissue. Various orthotopic models have been developed ***(14–19)***, but they are more labor-intensive and generally do not allow the accurate assessment of tumor growth and/or response unless investigators have access to small-animal cross-sectional imaging ***(20–22)***. Small-animal magnetic resonance imaging (MRI) allows assessing growth and response of intracavitary tumors ***(20–23)***, but the cost and labor-intensive nature of MRI limits its widespread use in preclinical drug testing. However, in brain tumors, where alternatives for assessing tumor response are limited, small animal MRI may see wider application. Micro-computerized tomography (CT) offers another means of assessing intracavitary lesions ***(24,25)***, but it is not suitable for intracranial lesions, and the time involved in obtaining and processing images prevents the routine use of micro-CT in drug testing.

Transduction of tumor cells with green fluorescent protein (GFP) is one method for assessing tumor growth and response by use of fluorescence imaging systems that can detect and quantify tumor masses in animals ***(26–28)***. However, the potential for GFP transduction to introduce artifacts is considerable, and GFP transduction has been shown to induce oxidative stress and to sensitize tumor cells to a variety of chemotherapeutic drugs ***(29)***. An alternative to GFP is to transduce tumor cells with firefly luciferase, which allows the light generated in tumors when the mice are given luciferin to be imaged in special devices ***(30–33)***. The potential for luciferase transduction to interfere with tumor growth or sensitize tumor cells to chemotherapy remains unknown. Also, because of the induction of an immune response, either luciferase or GFP marking is limited to use in immunocompromised mice.

Analysis of progression-free survival provides one alternative to intracavitary imaging, but the lack of tumor response data and the inability to exclude tumors that do not engraft from the analysis diminish the usefulness of such models. However, when employing disseminated disease models (tail vein injection)

for solid tumors or for leukemias, progression-free survival remains the primary approach for assessing the response of disseminated disease ***(9–11,34,35)***.

For tumors in which intravenous injection of tumor cells causes pulmonary or bone metastases, relatively inexpensive analog radiological methods can provide a means of documenting tumor engraftment prior to therapeutic studies, and may also be used to assess response. Intravenous injection or direct injection of some tumor cell lines into the femur or tibia of mice produces bone invasion that can cause lytic lesions evauable with analog radiology ***(36)***. Such bone invasion and/or metastasis models have been developed for breast cancer ***(37–39)***, prostate cancer ***(40)***, and neuroblastoma ***(41)***. These models are useful for testing agents that have direct antitumor effects, or agents (such as bisphosphonates) that retard or prevent skeletal events.

We will review here methods for assessing tumor progression and response in subcutaneous murine models with direct measurement. We will also review radiographic techniques currently under development that can be used to assess tumor progression and response to therapy without the use of potentially artifact-inducing transduced cell markers.

2. Materials

1. *Mice*. Mice (female, 4–6-wk-old athymic balb/c *(nu/nu)* or homozygous SCID C.B-17/IcrHsd-scid mutant mice can be obtained from a variety of vendors. Mice should be allowed to acclimate to their new environment for 1 wk after arrival.
2. *Animal caging.* Cages require a laminar-flow air delivery system (such as that made by Lab Products, Seaford, DE) or filter cage bonnets on polycarbonate microisolator cages lined with autoclaved bedding to maintain an aseptic environment. Mice should be maintained according to Institutional Animal Care and Use Committee (IACUC) approved experimental protocols. Autoclaved and acidified (pH = 4–6) water and autoclaved standard Purina mouse chow should be provided *ad libitum.*
3. *Medium for suspending tumor cells.* To minimize pH changes during handling of cells outside of a CO_2 incubator and to decrease clumping (especially deleterious with intravenous injections), cells are optimally suspended in L-15 (non-bicarbonate-based, non-CO_2-requiring medium) that is made without calcium or magnesisum.
4. *Calipers.* Although vernier and dial calipers can be used for measuring subcutaneous tumors, digital calipers (such as those made by Fisher Scientific, Tustin, CA) are the most suitable for the task. Systems for direct entry of caliper data into microcomputers have also been developed ***(42)***. However, employing two individuals for the measurements (one to measure, one to transcribe) allows rapid collection of data without the use of computerized calipers.
5. *Injectable anesthetics.* Pentobarbital sodium injection (Abbott Laboratories, North Chicago, IL), given ip at 40 mg/kg is one means of anesthesia. Another is an ip injection of 2.5% Avertin, 0.02 mL 2.5% Avertin/g body weight (ip) for mice,

with a 100% stock solution consisting of 1 g of 2,2,2-tribromoethanol in 1 mL *tert*-amyl alcohol (both made by Sigma-Aldrich, Milwaukee, WI). Mice can also be anesthetized by ip injection of a mixture of ketamine (50 mg/kg) and xylocaine (5 mg/kg).

6. *Inhalational anesthesia.* Isoflurane anesthetic + oxygen is delivered from an inhalational anesthetic apparatus (Abbott Laboratories, North Chicago, IL).
7. *Animal temperature control system.* To prevent hypothermia, one must provide temperature control for the mice during anesthesia. A suitable system for doing this is a water heating pad, the heat therapy system, comprised of a pad (REF TP22GT/PAD) and a pump (T/Pimp TP 500/TP500 C), both made by Gaymar Industries, Orchard Park, NY.
8. *Radiographic system.* Radiographs are generated using a Faxitron MX-20 small-animal X-ray device (Faxitron X-ray Corp., Wheeling, IL). To provide high-resolution radiographs, mammography computed radiography cassettes with high-resolution screens and high-detail single-emulsion mammography film and screens (Fuji EC-MA cassette, Fuji Photo Film Co., Japan) are used ***(41)***. Mammography products from other vendors are likely to give similar results.
9. *Software.* Tumor volume measurements, averages and standard deviations, and differences between treated and control animals can be calculated using Microsoft Excel. This program can also be used for creating rudimentary tumor growth-over-time graphs. Macros developed in Excel can also be used to generate Kaplan-Meier (log-rank) assessment of time to progression. Analyzed data can be copied from Excel to SigmaPlot (Jandell Scientific, San Rafael, CA) to create publication-quality graphics.

3. Methods

3.1. Maintaining Immunocompromised Mice

Mice are allowed to acclimate to their new environment for 1 wk after arrival. Mice are handled under strict aseptic conditions, opening the cage in a laminar-flow hood while wearing a sterile gown and gloves.

3.2. Establishing Subcutaneous Xenografts

1. Harvest cells that are 75–80% confluent, highly viable, and in logarithmic growth phase. It is preferred to grow cells in antibiotic-free medium to avoid masking microbial contamination. For neuroblastoma, rhabdomyosarcoma, Ewing's family tumors, retinoblastoma, and certain other tumor types we find that cells can be removed from the substrate using Puck's Solution A plus EDTA (Puck's EDTA), which contains 140 m*M* NaCl, 5 m*M* KCl, 5.5 m*M* glucose, 4 m*M* $NaHCO_3$, 0.8 m*M* ethylenediaminetetraacetic acid (EDTA), 13 μ*M* phenol red, and 9 m*M* HEPES buffer (pH 7.3) ***(43)***, thus avoiding the additional cell damage from trypsin.
2. Viable cell number is determined by hemocytometer counting using trypan blue, and 5–50 million tumor cells (depending on tumorigencity and growth rate) are

injected subcutaneously between the shoulder blades of three to five athyhmic (*nu/nu*) mice using strict aseptic technique, with a 1-cm^3-syringe and a 19-gage needle.
3. For injection, cells are suspended in L-15 medium (Ca^{2+}/Mg^{2+}-free) culture medium without fetal bovine serum (FBS) such that a total of 200 µL are injected to deliver the desired cell dose.
4. Mice are observed biweekly and tumor growth monitored when tumors become palpable; the lag phase varies from 2 to 12 weeks, depending on the amount of cells injected, the tumor type, and the cell line employed.
5. When tumors reach about 1.5 cm^3, two to four mice are sacrificed, the skin over the tumor disinfected with betadine, and the tumors removed under aseptic conditions.
6. The tumor cells are forced through a sterile 80–160-µm stainless-steel mesh strainer, and mixed with cell culture medium to form a slurry, such that injection of 200 µL subcutaneously between the shoulder blades of 20–25 mice delivers a tumor cell dose of approx 5–50 million cells, depending on how aggressive the tumor is (*see* **Note 1**).

3.3. Assessing the Volume of Subcutaneous Tumors by Caliper Measurements

1. Tumors should be measured beginning when they are first palpable: the length (L = longest dimension), the width (W = the distance perpendicular to and in the same plane as the length), and the height (H = the distance between the exterior tumor edge and the mouse body). The ellipsoid volume of the tumor, calculated from $0.5 \times L \times W \times H$, provides the most accurate measure of tumor mass ***(13)*** **(Fig. 1)**.
2. For multilobed tumors, or those that grow in irregular shapes, the tumor should be divided visually into two, three, or four lobes of similar dimension that are measured separately **(Fig. 1)**. The calculated volume for each lobe can be summed to obtain the volume of the entire mass ***(13)***.

3.4. Establishing Pulmonary and Bone Metastases by Intravenous Injection

1. Cells are harvested from tissue culture flasks, counted, and suspended in serum-free L-15 (calcium- and magnesium-free) medium at a concentration of 20×10^6 cells/mL.
2. The mouse should be gently warmed using a heat lamp to increase tail vein circulation, then placed in a suitable restrainer ***(10)***, and the tail prepared with betadine and 70% alcohol.
3. The cell suspension is placed into a 1-mL syringe and 100 µL of the cell suspension is injected through a 30-gage needle into the lateral tail vein.

3.5. Small Animal Anesthesia **(44)** *(***see** *Note 2)*

1. Turn on the oxygen tank. Check the tank meter to ensure that it reads between full and the top of the refill area (red).

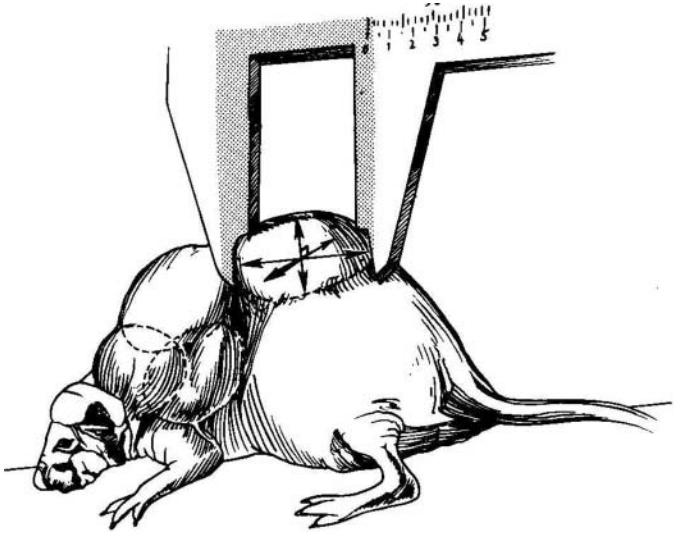

Fig. 1. Illustration of the method for measuring subcutaneous tumors in mice. Tumors are measured in three dimensions, the length (longest dimension), width (shorter dimension, perpendicular to the length), and height (diameter of tumor perpendicular to the length and the width. For multilobed tumors, individual lobes can be measured separately and summed to derive the entire tumor mass.

2. To begin the procedure the oxygen flow meter (green knob on left side of machine) must read 1 L.
3. Turn on (press button) isoflurane vaporizer to achieve 5% for induction. Closely observe the animal and continue until breathing is slow (appropriate anesthesia generally reached within 1 min).
4. After induction, reduce the isoflurane to 2.5% for maintenance of the anesthesia, adjust as necessary, and constantly monitor animals for breathing.
5. To prevent hypothermia, animals must be placed on a body-temperature controller until recovered from the anesthesia.
6. Mice can also be anesthetized by ip injection of a mixture of ketamine (50 mg/kg) and xylocaine (5 mg/kg), or by an ip injection of 2.5% Avertin (300 µL per 25-g mouse body weight). Pentobarbital sodium injection given ip at 40 mg/kg provides a suitable alternative.

3.6. Establishing Invasive Bone Tumors by Direct Injection

1. Injection of certain tumor cell lines into the femur or tibia of immunocompromised mice can result in osteolytic lesions ***(40,41)***.
2. To implant cells into the femur, anesthetized mice are placed in a lateral position and the skin overlying the knee and femur cleansed with betadine.

3. A small incision (8–10 mm) is made along the right knee, and the patellar tendon and muscle are split longitudinally to expose the distal femur.
4. A surgical scalpel tip or a 26-gage needle (stabilized with a drill holder) is used to drill a tiny hole in the cortex of the bone.
5. Tumor cells (1×10^5/μL) are suspended in cell culture medium (without FBS) and 2–5 μL of medium + tumor cells are injected into the bone marrow space slowly via a 30-gage sterile needle attached to a Hamilton 10-μL syringe (Hamilton, Reno, NV).
6. The position of the needle in the marrow cavity can be confirmed by translumination.
7. After injection, the needle is removed and the hole is sealed with bone wax, the patellar tendon reapproximated, and the skin closed with cyanoacrylate (Nexaband, Veterinary Products Lab, Phoenix, AZ).
8. Mice must be monitored carefully for signs of discomfort, and analgesics can be used immediately after initial surgery and at other times as indicated. Mice are euthanized if they show signs of significant discomfort.
9. A less labor-intensive approach involves injection into the tibia of the mouse, which requires anesthesia but no incision. Mice are maintained under isoflurane anesthesia during the tumor injection procedure.
10. The hair is shaved around the injection site and the skin surface at the injection site is prepped with betadine scrub followed by a 70% alcohol wipe.
11. A 25- or 26-gauge needle is inserted into the proximal joint of the tibia (through the tibial crest) to provide access to the bone marrow and is then removed.
12. Cells (also suspended in serum-free medium at 1×10^5 μL) are then injected (~2–5 μL) into the marrow cavity of the right hind leg tibial metaphysis, using a 30-gage needle attached to a Hamilton 10-μL syringe.

3.7. Determination of Therapeutic Effect in Murine Tumor Models (see Note 3)

Regardless of whether survival data or tumor measurements are the primary end points, mice should be weighed throughout the course of the experiments, as body weight provides another means of assessing toxicity, usually done in terms of percentage change of body weight from the weight at start of the experiment. Here we will summarize approaches to measuring antitumor effect in both subcutaneous and disseminated disease models, which have been reviewed extensively elsewhere ***(2,35,45)***.

3.7.1. Intracavitary or Disseminated Disease Models

These models are attractive in that the tumor cells are often growing in physiologically more relevant tissues than is a subcutaneous xenograft. However, the difficulty (and often impossibility) of measuring the tumor prevents a serial determination of tumor progressive growth in treated vs control animals.

1. Assessing disease burden in leukemia or neuroblastoma can be done using flow cytometry or polymerase chain reaction (PCR) from serial blood samples ***(10,34,46)***.
2. Nonetheless, the general end point remains survival from initiation of experiment until the animal is distressed or moribund (*see* **Note 4**).

3.7.2. Measures of Antitumor Effect in Disseminated Models

1. Percentage mean or median increase in life span = ratio of the survival time in days of treated animals to the survival time of the untreated control animals. This can be determined as percentage increase in lifespan (% ILS), which is calculated in days from initiation until a moribund state (or death) for treated vs control as % ILS = $[(T - C) / C] \times 100$ ***(7)***.
2. An alternative to this is to calculate a T / C ratio for days of survival (or lack of progression).
3. Kaplan-Meier (log-rank) survival analysis can be utilized ***(47)***.
4. Net $\log_{10}$ cell kill = $T - C$ – (duration of treatment in days) / $3.32 \times T_d$. $T - C$ is the difference in the median day of death (moribund state) between the treated (T) and the control (C) cohorts ***(7)***. The constant 3.32 is the number of doublings required for a population to increase on $\log_{10}$ unit, and T_d is the mean doubling time of the tumor in days, calculated from a log-linear least-squares fit of tumor growth. For disseminated disease models, the latter value is difficult and perhaps impossible to obtain accurately.

3.7.3. Subcutaneous Tumor Models

These models have the advantages of (1) providing visual confirmation that 100% of the mice used in an experiment have tumors prior to therapy; and (2) providing a means of assessing tumor response or growth over time, with the latter providing more information than the increase in animal survival that can be measured in intracavitary models.

1. Subcutaneous tumor volumes should be measured as described under **Subheading 3.7.**
2. Data should be presented graphically as shown in **Fig. 2**, in which the growth over time for each mouse in the treated and control groups is shown. Averages of these data can also be displayed or calculated, but it is essential to present each of the mice separately to allow a full assessment of the data ***(45)***. Some investigators prefer to do this on a linear scale, while others prefer a semilog scale.
3. For subcutaneous tumors, some experiments involve treating the mice prior to documentation of growing, progressing tumors. These “tumor growth delay” experiments suffer from the same need for high-take rates or large numbers of mice that was discussed under intracavitary models. Again, cross-sectional imaging may prove useful in defining the presence of disease in such models.
4. For models in which treatment begins after tumor growth is documented, often when tumors are at a size of 30–100 mm^3, usually two measurements showing

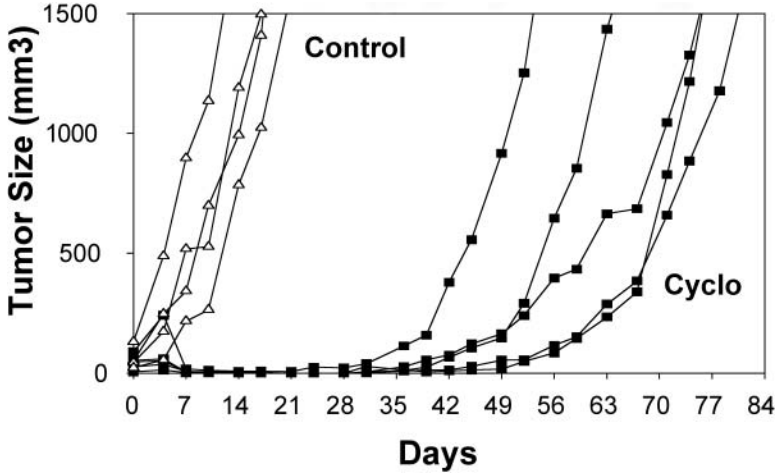

Fig. 2. Example of antitumor activity against a subcutaneous tumor xenograft from the CHLA-136 neuroblastoma cell line ***(52)*** in a nude mouse as assessed by serial measurements of tumor volume. Each line represents the tumor growth over time for an individual mouse. Shown are control mice (△) and mice treated for 5 d with daily injections (ip) of 156 mg/kg of cyclophosphamide (■).

increasing tumor size prior to therapy are sufficient to establish tumor engraftment and progression.

5. Tumor volume should be measured twice weekly. The *T/C* ratio can be calculated as a T/C ratio = days to obtain a predefined tumor mass for the treated animals divided by the days to obtain the same size mass in the control animals. For example, with the data shown in **Fig. 2**, the T/C ratio was 3.9.
6. In addition, because the treated animals had a prolonged period without tumor progression, one could also calculate the median time to progression (TTP) at 31 d for the treated animals vs 3 d (first documented progression) for the controls.
7. Data can also be presented as a percent increase in lifespan (% ILS), which is calculated in days from initiation until a moribund state (or death) for treated vs control as % ILS = $[(T - C) / C] \times 100$ ***(7)***.
8. Kaplan-Meier (log-rank) analysis of survival or time to progression can also be calculated ***(47)***.
9. Analyzing growth of tumors over time has been done using a variety of mathematical approaches ***(48–51)***. Although complex models (such as those employing the Gompertz function) are useful for studying growth properties and kinetics of xenografted tumors, they are not generally needed for assessing response to therapy, or in determination of xenograft doubling time, as the latter can usually be done accurately by linear regression ***(51)***.

10. For subcutaneously growing tumors, a $\log_{10}$ cell kill can also be calculated as follows:

$$\log_{10} \text{ cell kill} = (T - C \text{ value in days}) / (3.32)(T_d)$$

where $T - C$ (tumor growth delay) = days to reach a defined mass for the treated animals – days to reach the same mass for the control animals; 3.32 is the $\log_{10}$ unit constant; T_d is the doubling time for the tumor in days (derived from the doubling time of the control tumors using a $\log_2$ (linear regression) formula ***(51)***.

3.8. Radiographic Assessment of Pulmonary Lesions

1. Mice are anesthesized under aseptic conditions and then are placed into Ziplock plastic sandwich bags to provide an aseptic barrier.
2. The Ziplock bags are sealed such that a pocket of the isofluorene/O_2 mixture is contained in the bag, providing sufficient gas for the few minutes needed to complete the X-ray.
3. To provide a magnification factor for the radiographs, mice are positioned 10.5 cm below the radiation source, and the film placed at the bottom of the Faxitron, 37.5 cm below the animal. This approach provides a magnification factor of 4 times, with the thoracic cavity of the mouse filling about half the area of the 18×24-cm mammography film. An example of pulmonary metastases from intravenous injection of a primitive neuroectodermal tumor (PNET) cell line in a SCID mouse is shown in **Fig. 3**.

3.9. Radiographic Assessment of Bone Lesions

1. To image bone lesions (direct-injection invasive lesions or metastases), radiographic procedures identical to those described for pulmonary lesions are employed, except that the mouse is positioned to ensure imaging of the lower portion of the mouse, including both legs.
2. We have developed a grading system for bone lesions in mice given direct tumor injection into the femur that provides quantitative scoring of the bone lesions (*see* **Note 5**). The grading system defines four grades: Grade 1 represents a normal bone when compared to the contralateral bone. Grade 2 lesions are asymmetric (relative to contralateral bone) and progressive radiolucent lesions limited to the site of injection. Grade 3 shows asymmetrical and progressive radiolucent areas extending beyond the distal femur. Grade 4 lesions contain a pathological fracture of the bone or a breach in the bone cortex.
3. The time to develop a Grade 4 lesion can be used as a relative end point to determine tumor progression and/or response to therapy ***(41)***. An example of a lytic bone lesion from direct injection of a prostate cancer cell line into an athymic mouse is shown in **Fig. 4**.

4. Notes

1. Transfer of tumors in this fashion can be repeated many times, but to avoid genetic drift from the original cell line one should limit such transfers to six or less.

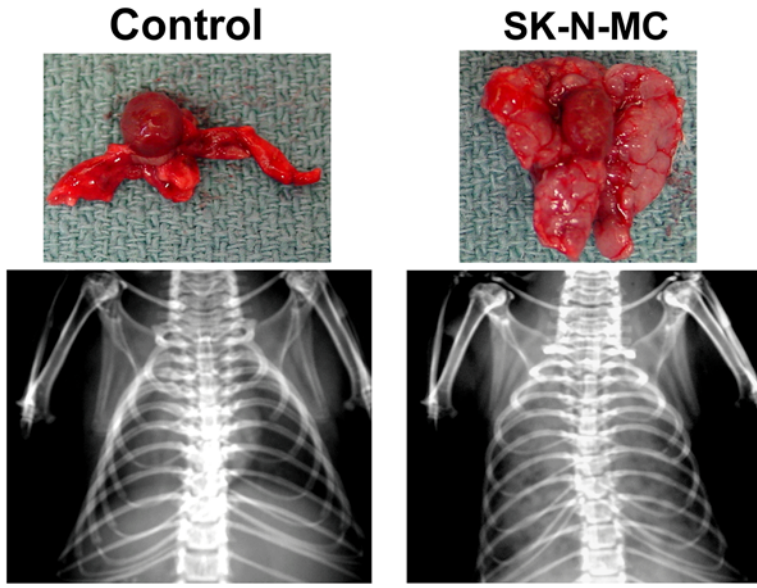

Fig. 3. Radiographic demonstration of experimental pulmonary metastases in a SCID mouse. Mice were injected in the lateral tail vein with 2×10^6 cells from the SK-N-MC primitive neuroectodermal tumor cell line ***(53)***. After 8 wk, multiple pulmonary metastases can be visualized by Faxitron X-ray, which were not seen in the control mice. Postmortem examination confirmed that the lesions seen by X-ray were indeed multiple tumor nodules, visible on gross examination (right panel) and by histopathology (not shown).

2. Ensure that all instruments, animals, and caging are fully prepared before initiating the procedure. Check valves of all tubes and assure open air flow.
3. One approach in the past to measuring a therapeutic effect of a drug was to establish a tumor and then compare survival of treated to untreated mice. However, using actual survival as an end point is no longer acceptable, and mice that become distressed, or in particular those that are moribund, must be euthanized. Similarly, in the case of animals bearing subcutaneous tumors, when a predetermined tumor size (usually for mice this is a tumor > 1500 mm^3) is reached, the animal must be sacrificed. Thus, all survival data for subcutaneous tumors will reflect a combination of death for toxicity (or other events) and attaining a certain tumor size. By contrast, intracavitary or disseminated disease models will measure survival until death from toxicity, other events, or observation of obvious distress or a moribund state. Death of a treated animal should be presumed to be treatment-related if the animal dies within 15 d of the last therapy, unless death appears to be from tumor progression.
4. A secondary problem with these models is the need for a very high (ideally 100%) success rate for engrafting tumor. The high “take rate” is needed because even a

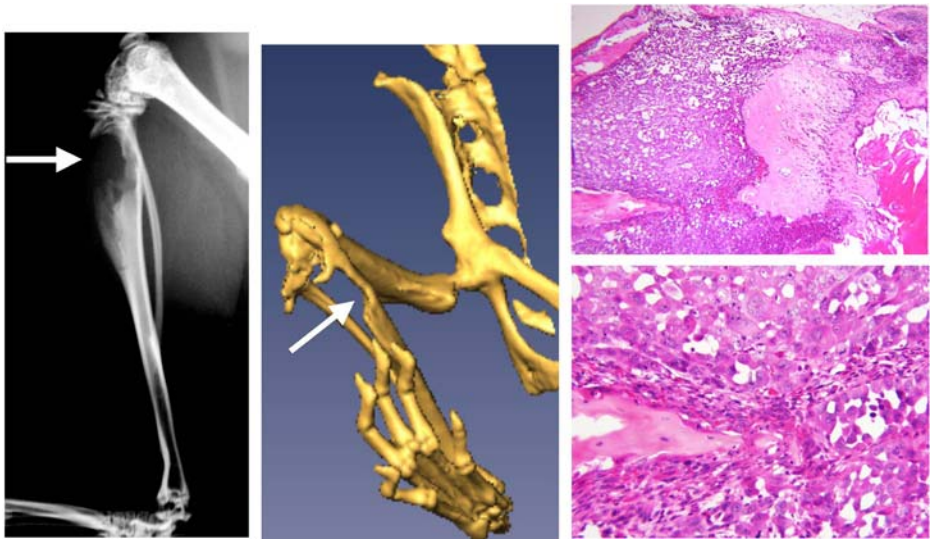

Fig. 4. Lytic lesion in bone of a SCID mouse given an intra-tibial injection of the PC-3 human prostate cancer cell line. Image in left panel from the Faxitron small-animal imager with high-resolution mammography film, middle panel is a 3-D reconstruction of the same lesion from the Micro-Cat CT system. Arrows point to the lytic lesion. Histology (low and high magnification) from the same lesion is shown in the right panel. (Histology photomicrographs courtesy of Hiro Shimada, MD.)

95% "take rate" can result in the need for very large numbers of mice in any given therapeutic experiment to achieve statistical validity. One approach to overcome this problem would be the use of cross-sectional imaging to confirm disease (in a single observation) prior to starting therapy.

5. The scale is not independent of mouse strain especially at low values, i.e., values of 1 and 2. Thus, care should be taken to customize the scale for your particular strain.

Acknowledgments

This work was supported in part by the Neil Bogart Memorial Laboratories of the T. J. Martell Foundation for Leukemia, Cancer, and AIDS Research, and by National Cancer Institute Grants CA82830, CA81403, and CA102990.

References

1. Corbet, T. H., Polin, L., Roberts, B. J., et al. (2002) Transplantable syngeneic rodent tumors: solid tumors in mice, in *Tumor Models in Cancer Research* (Teicher, B. A., ed.), Humana Press, Totowa, NJ, pp 41–71.
2. Harrison, S. (2002) Perspective on the history of tumor models, in *Anticancer Drug Development Guide* (Teicher, B. A., ed.), Humana Press, Totowa, NJ, pp. 3–19.

3. Waud, W. R. (1997) Murine L1210 and P388 leukemias, in *Anticancer Drug Development Guide: Preclinical Screening, Clinical Trials, and Approval* (Teicher, B. A., ed.), Humana Press, Totowa, NJ, pp. 59–74.
4. Fiebig, H. H. and Burger, A. M. (2002) Human tumor xenografts and explants, in *Tumor Models in Cancer Research* (Teicher, B. A., ed.), Humana Press, Totowa, NJ, pp. 113–137.
5. Mattern, J., Bak, M., Hahn, E. W., and Volm, M. (1988) Human tumor xenografts as model for drug testing. *Cancer Metastasis Rev.* **7,** 263–284.
6. Houghton, P. J., Adamson, P. C., Blaney, S., et al. (2002) Testing of new agents in childhood cancer preclinical models: meeting summary. *Clin. Cancer Res.* **8,** 3646–3657.
7. Plowman, J., Dykes, D. J., Hollingshead, M., Simpson-Herren, L., and Alley, M. C. (1997) Human tumor xenograft models in NCI drug development, in *Anticancer Drug Development Guide: Preclinical Screening, Clinical Trials, and Approval* (Teicher, B. A., ed.), Humana Press, Totowa, NJ, pp. 101–125.
8. Shimosato, Y., Kameya, T., and Hirohashi, S. (1979) Growth, morphology, and function of xenotransplanted human tumors. *Pathol. Annu.* **14(pt 2),** 215–257.
9. Lock, R. B., Liem, N., Farnsworth, M. L., et al. (2002) The nonobese diabetic/severe combined immunodeficient (NOD/SCID) mouse model of childhood acute lymphoblastic leukemia reveals intrinsic differences in biologic characteristics at diagnosis and relapse. *Blood* **99,** 4100–4108.
10. Lock, R. B., Liem, N. L., and Papa, R. A. (2005) Preclinical testing of anti-leukemic drugs using an in vivo model of systemic disease. *Chemosensitivity; Volume 2. In Vivo Models, Imaging, and Molecular Regulators* (Blumenthal, R. D., ed.), Humana, Totowa, NJ (in press, this volume).
11. Lehne, G., Sorensen, D. R., Tjonnfjord, G. E., et al. (2002) The cyclosporin PSC 833 increases survival and delays engraftment of human multidrug-resistant leukemia cells in xenotransplanted NOD-SCID mice. *Leukemia* **16,** 2388–2394.
12. Johnson, J. I., Decker, S., Zaharevitz, D., et al. (2001) Relationships between drug activity in NCI preclinical in vitro and in vivo models and early clinical trials. [see comment]. *Br. J. Cancer* **84,** 1424–1431.
13. Tomayko, M. M. and Reynolds, C. P. (1989) Determination of subcutaneous tumor size in athymic (nude) mice. *Cancer Chemother. Pharmacol.* **24,** 148–154.
14. Manzotti, C., Audisio, R. A., and Pratesi, G. (1993) Importance of orthotopic implantation for human tumors as model systems: relevance to metastasis and invasion. *Clin. Exp. Metastasis* **11,** 5–14.
15. Kubota,T. (1994) Metastatic models of human cancer xenografted in the nude mouse: the importance of orthotopic transplantation. *J. Cell. Biochem.* **56,** 4–8.
16. Khanna, C., Jaboin, J. J., Drakos, E., Tsokos, M., and Thiele, C. J. (2002) Biologically relevant orthotopic neuroblastoma xenograft models: primary adrenal tumor growth and spontaneous distant metastasis. *In Vivo* **16,** 77–85.
17. Khanna, C., Prehn, J., Yeung, C., Caylor, J., Tsokos, M., and Helman, L. (2000) An orthotopic model of murine osteosarcoma with clonally related variants differing in pulmonary metastatic potential. *Clin. Exp. Metastasis* **18,** 261–271.

18. Shoji, T., Konno, H., Tanaka, T., et al. (2003) Orthotopic implantation of a colon cancer xenograft induces high expression of cyclooxygenase-2. *Cancer Lett.* **195,** 235–241.
19. El Galley, R., Keane, T. E., and Sun, C. (2003) Camptothecin analogues and vinblastine in the treatment of renal cell carcinoma: an in vivo study using a human orthotopic renal cancer xenograft. *Urol. Oncol.* **21,** 49–57.
20. Kikuchi, E., Xu, S., Ohori, M., et al. (2003) Detection and quantitative analysis of early stage orthotopic murine bladder tumor using in vivo magnetic resonance imaging. *J. Urol.* **170,** 1375–1378.
21. Moats, R., Ma, L. Q., Wajed, R., et al. (2000) Magnetic resonance imaging for the evaluation of a novel metastatic orthotopic model of human neuroblastoma in immunodeficient mice. *Clin. Exp. Metastasis* **18,** 455–461.
22. Grimm, J., Potthast, A., Wunder, A., and Moore, A. (2003) Magnetic resonance imaging of the pancreas and pancreatic tumors in a mouse orthotopic model of human cancer. *Int. J. Cancer* **106,** 806–811.
23. Nelson, A. L., Algon, S. A., Munasinghe, J., et al. (2003) Magnetic resonance imaging of patched heterozygous and xenografted mouse brain tumors. *J. Neuro-Oncol.* **62,** 259–267.
24. Paulus, M. J., Gleason, S. S., Easterly, M. E., and Foltz, C. J. (2001) A review of high-resolution X-ray computed tomography and other imaging modalities for small animal research. [Erratum appears in *Lab Anim* (NY) 2001 May;30(5):13]. *Lab Anim* **30,** 36–45.
25. Paulus, M. J., Gleason, S. S., Kennel, S. J., Hunsicker, P. R., and Johnson, D. K. (2000) High resolution X-ray computed tomography: an emerging tool for small animal cancer research. *Neoplasia* (NY) **2,** 62–70.
26. Ito, S., Nakanishi, H., Ikehara, Y., et al. (2001) Real-time observation of micrometastasis formation in the living mouse liver using a green fluorescent protein gene-tagged rat tongue carcinoma cell line. [Erratum appears in *Int. J. Cancer* 2002 Feb 20;97(6):878]. *Int. J. Cancer* **93,** 212–217.
27. Hoffman, R. M. (1024) Visualization of GFP-expressing tumors and metastasis in vivo. *Biotechniques* **30,** 1016–1022.
28. Yang, M., Baranov, E., Jiang, P., et al. (2000) Whole-body optical imaging of green fluorescent protein-expressing tumors and metastases. *Proc. Natl. Acad. Sci. USA* **97,** 1206–1211.
29. Goto, H., Yang, B., Petersen, D., et al. (2003) Transduction of green fluorescent protein increased oxidative stress and enhanced sensitivity to cytotoxic drugs in neuroblastoma cell lines. *Mol. Cancer Ther.* **2,** 911–917.
30. Zhang, L., Hellstrom, K. E., and Chen, L. (1994) Luciferase activity as a marker of tumor burden and as an indicator of tumor response to antineoplastic therapy in vivo. *Clin. Exp. Metastasis* **12,** 87–92.
31. Rice, B. W., Cable, M. D., and Nelson, M. B. (2001) In vivo imaging of light-emitting probes. *J. Biomed. Optics* **6,** 432–440.

32. Edinger, M., Sweeney, T. J., Tucker, A. A., Olomu, A. B., Negrin, R. S., and Contag, C. H. (1999) Noninvasive assessment of tumor cell proliferation in animal models. *Neoplasia* (NY) **1,** 303–310.
33. El Hilali, N., Rubio, N., Martinez-Villacampa, M., and Blanco, J. (2002) Combined noninvasive imaging and luminometric quantification of luciferase-labeled human prostate tumors and metastases. *Lab. Invest.* **82,** 1563–1571.
34. Thompson, J., Guichard, S. M., Cheshire, P. J., et al. (2001) Development, characterization and therapy of a disseminated model of childhood neuroblastoma in SCID mice. *Cancer Chemother. Pharmacol.* **47,** 211–221.
35. Teicher, B. A. (2002) In vivo tumor response end points, in *Tumor Models in Cancer Research* (Teicher, B. A., ed.), Humana Press, Totowa, NJ, pp. 593–616.
36. Menon, K. and Teicher, B. A. (2002) Metastasis models Lungs, spleen/liver, bone, brain, in *Tumor Models in Cancer Research* (Teicher, B. A., ed.), Humana Press, Totowa, NJ, pp. 277–291.
37. Iwasaki, T., Mukai, M., Tsujimura, T., et al. (2002) Ipriflavone inhibits osteolytic bone metastasis of human breast cancer cells in a nude mouse model. *Int. J. Cancer* **100,** 381–387.
38. Yi, B., Williams, P. J., Niewolna, M., Wang, Y., and Yoneda, T. (2002) Tumor-derived platelet-derived growth factor-BB plays a critical role in osteosclerotic bone metastasis in an animal model of human breast cancer. *Cancer Res.* **62,** 917–923.
39. Peyruchaud, O., Winding, B., Pecheur, I., Serre, C. M., Delmas, P., and Clezardin, P. (2001) Early detection of bone metastases in a murine model using fluorescent human breast cancer cells: application to the use of the bisphosphonate zoledronic acid in the treatment of osteolytic lesions. *J. Bone Miner. Res.* **16,** 2027–2034.
40. Corey, E., Quinn, J. E., Bladou, F., et al. (2002) Establishment and characterization of osseous prostate cancer models: intra-tibial injection of human prostate cancer cells. *Prostate* **52,** 20–33.
41. Sohara, Y., Shimada, H, Scadeng, M, et al. (2003) Lytic bone lesions in a human neuroblastoma xenogaft show osteo-clast recruitment and are inhibited by ibandronate. *Cancer Res.* **63,** 3026–3031.
42. Worzalla, J. F., Bewley, J. R., and Grindey, G. B. (1990) Automated measurement of transplantable solid tumors using digital electronic calipers interfaced to a microcomputer. *Invest. New Drugs* **8,** 241–251.
43. Reynolds, C. P., Biedler, J. L., Spengler, B. A., et al. (1986) Characterization of human neuroblastoma cell lines established before and after therapy. *J. Natl. Cancer Inst.* **76,** 375–387.
44. Meyer, R. E., Braun, R. D., and Dewhirst, M. W. (2002) Anesthetic considerations for the study of murine tumor models, in *Tumor Models in Cancer Research* (Teicher, B. A., ed.), Humana Press, Totowa, NJ, pp. 407–431.
45. Begg, A. C. (1980) Analysis of growth delay data: potential pitfalls. *Br. J. Cancer Suppl.* **41,** 93–97.

46. Dialynas, D. P., Shao, L., Billman, G. F., and Yu, J. (2001) Engraftment of human T-cell acute lymphoblastic leukemia in immunodeficient NOD/SCID mice which have been preconditioned by injection of human cord blood. *Stem Cells* **19,** 443–452.
47. Fleming, T. R. and Lin, D. Y. (2000) Survival analysis in clinical trials: past developments and future directions. *Biometrics* **56,** 971–983.
48. G. Gordon Steel. (1977) *Growth Kinetics of Tumoours Cell Population Kinetics in Relations to the Growth and Treatment of Cancer.* Clarendon Press, Oxford.
49. Demicheli, R., Pratesi, G., and Foroni, R. (1991) The exponential-Gompertzian tumor growth model: data from six tumor cell lines in vitro and in vivo. Estimate of the transition point from exponential to Gompertzian growth and potential clinical implications. *Tumori* **77,** 189–195.
50. Rygaard, K. and Spang-Thomsen, M. (1997) Quantitation and gompertzian analysis of tumor growth. *Breast Cancer Res. Treatment* **46,** 303–312.
51. Zwicker, J. I., Proffitt, R. T., and Reynolds, C. P. (1996) A microcomputer program for calculating cell population doubling time in vitro and in vivo. *Cancer Chemother. Pharmacol.* **37,** 203–210.
52. Keshelava, N., Zuo, J. J., Chen, P., et al. (2001) Loss of p53 function confers high-level multi-drug resistance in neuroblastoma cell lines. *Cancer Res.* **61,** 5103–5105.
53. Wang, Y., Einhorn, P., Triche, T. J., Seeger, R. C., and Reynolds, C. P. (2000) Expression of protein gene product 9.5 and tyrosine hydroxylase in childhood small round cell tumors. *Clin. Cancer Res.* **6,** 551–558.

Chemosensitivity

METHODS IN MOLECULAR MEDICINE™

John M. Walker, SERIES EDITOR

118 **Antifungal Agents:** *Methods and Protocols,* edited by *Erika J. Ernst and P. David Rogers, 2005*

117 **Fibrosis Research:** *Methods and Protocols,* edited by *John Varga, David A. Brenner, and Sem H. Phan, 2005*

116 **Inteferon Methods and Protocols**, edited by *Daniel J. J. Carr, 2005*

115 **Lymphoma:** *Methods and Protocols,* edited by *Timothy Illidge and Peter W. M. Johnson, 2005*

114 **Microarrays in Clinical Diagnostics**, edited by *Thomas Joos and Paolo Fortina, 2005*

113 **Multiple Myeloma:** *Methods and Protocols,* edited by *Ross D. Brown and P. Joy Ho, 2005*

112 **Molecular Cardiology:** *Methods and Protocols,* edited by *Zhongjie Sun, 2005*

111 **Chemosensitivity:** *Volume 2, In Vivo Models, Imaging, and Molecular Regulators,* edited by *Rosalyn D. Blumethal, 2005*

110 **Chemosensitivity:** *Volume 1, In Vitro Assays,* edited by *Rosalyn D. Blumethal, 2005*

109 **Adoptive Immunotherapy:** *Methods and Protocols,* edited by *Burkhard Ludewig and Matthias W. Hoffman, 2005*

108 **Hypertension:** *Methods and Protocols,* edited by *Jérôme P. Fennell and Andrew H. Baker, 2005*

107 **Human Cell Culture Protocols,** *Second Edition,* edited by *Joanna Picot, 2005*

106 **Antisense Therapeutics,** *Second Edition,* edited by *M. Ian Phillips, 2005*

105 **Developmental Hematopoiesis:** *Methods and Protocols,* edited by *Margaret H. Baron, 2005*

104 **Stroke Genomics:** *Methods and Reviews,* edited by *Simon J. Read and David Virley, 2004*

103 **Pancreatic Cancer:** *Methods and Protocols,* edited by *Gloria H. Su, 2004*

102 **Autoimmunity:** *Methods and Protocols,* edited by *Andras Perl, 2004*

101 **Cartilage and Osteoarthritis:** *Volume 2, Structure and In Vivo Analysis,* edited by *Frédéric De Ceuninck, Massimo Sabatini, and Philippe Pastoureau, 2004*

100 **Cartilage and Osteoarthritis:** *Volume 1, Cellular and Molecular Tools,* edited by *Massimo Sabatini, Philippe Pastoureau, and Frédéric De Ceuninck, 2004*

99 **Pain Research:** *Methods and Protocols,* edited by *David Z. Luo, 2004*

98 **Tumor Necrosis Factor:** *Methods and Protocols,* edited by *Angelo Corti and Pietro Ghezzi, 2004*

97 **Molecular Diagnosis of Cancer:** *Methods and Protocols, Second Edition,* edited by *Joseph E. Roulston and John M. S. Bartlett, 2004*

96 **Hepatitis B and D Protocols:** *Volume 2, Immunology, Model Systems, and Clinical Studies,* edited by *Robert K. Hamatake and Johnson Y. N. Lau, 2004*

95 **Hepatitis B and D Protocols:** *Volume 1, Detection, Genotypes, and Characterization,* edited by *Robert K. Hamatake and Johnson Y. N. Lau, 2004*

94 **Molecular Diagnosis of Infectious Diseases,** *Second Edition,* edited by *Jochen Decker and Udo Reischl, 2004*

93 **Anticoagulants, Antiplatelets, and Thrombolytics,** edited by *Shaker A. Mousa, 2004*

92 **Molecular Diagnosis of Genetic Diseases,** *Second Edition,* edited by *Rob Elles and Roger Mountford, 2004*

91 **Pediatric Hematology:** *Methods and Protocols,* edited by *Nicholas J. Goulden and Colin G. Steward, 2003*

90 **Suicide Gene Therapy:** *Methods and Reviews,* edited by *Caroline J. Springer, 2004*

89 **The Blood–Brain Barrier:** *Biology and Research Protocols,* edited by *Sukriti Nag, 2003*

88 **Cancer Cell Culture:** *Methods and Protocols,* edited by *Simon P. Langdon, 2003*

87 **Vaccine Protocols,** *Second Edition,* edited by *Andrew Robinson, Michael J. Hudson, and Martin P. Cranage, 2003*

86 **Renal Disease:** *Techniques and Protocols,* edited by *Michael S. Goligorsky, 2003*

85 **Novel Anticancer Drug Protocols,** edited by *John K. Buolamwini and Alex A. Adjei, 2003*

84 **Opioid Research:** *Methods and Protocols,* edited by *Zhizhong Z. Pan, 2003*

83 **Diabetes Mellitus:** *Methods and Protocols,* edited by *Sabire Özcan, 2003*

82 **Hemoglobin Disorders:** *Molecular Methods and Protocols,* edited by *Ronald L. Nagel, 2003*

METHODS IN MOLECULAR MEDICINE™

Chemosensitivity

Volume 2

In Vivo Models, Imaging, and Molecular Regulators

Edited by

Rosalyn D. Blumenthal

Garden State Cancer Center, Belleville, NJ

HUMANA PRESS TOTOWA, NEW JERSEY

999 Riverview Drive, Suite 208
Totowa, New Jersey 07512

www.humanapress.com

This publication is printed on acid-free paper. ∞
ANSI Z39.48-1984 (American Standards Institute)

Permanence of Paper for Printed Library Materials.

Cover illustrations: *Foreground illustration*: Figure 4, from Chapter 24, "^{99m}Tc-Annexin A5 Uptake and Imaging to Monitor Chemosensitivity," by Tarik Z. Belhocine and Francis G. Blankenberg. *Background illustration*: Figure 4, from Chapter 22 (Volume 2), "Assessing Growth and Response to Therapy in Murine Tumor Models," by C. P. Reynolds et al.

Cover design by Patricia F. Cleary.

For additional copies, pricing for bulk purchases, and/or information about other Humana titles, contact Humana at the above address or at any of the following numbers: Tel.: 973-256-1699; Fax: 973-256-8341; E-mail: humana@humanapr.com; or visit our Website: www.humanapress.com

Printed in the United States of America. 10 9 8 7 6 5 4 3 2 1

E-ISBN 1-59259-889-7
Library of Congress Cataloging in Publication Data
Chemosensitivity / edited by Rosalyn D. Blumenthal.
v. ; cm. — (Methods in molecular medicine ; 110-111)
Includes bibliographical references and index.
Contents: v. 1. In vitro assays — v. 2 In vivo models, imaging, and molecular regulators.
ISBN 1-58829-586-9 (hardcover : alk. paper)
1. Cancer—Chemotherapy—Laboratory manuals. 2. Antineoplastic agents—Effectiveness—Laboratory manuals. 3. Cancer cells—Laboratory manuals. 4. Cancer--Molecular aspects—Laboratory manuals. [DNLM: 1. Antineoplastic Agents—pharmacology. 2. Drug Screening Assays, Antitumor—methods. 3. Drug Resistance, Neoplasm. 4. Models, Animal. 5. Neoplasms—drug therapy. QV 269 C5177 2005] I. Blumenthal, Rosalyn D. II. Series.

RC271.C5C396 2005

616.99'4061—dc22 2004012494

Preface

Chemotherapy is used to treat many types of cancer. A large number of drug classes are in use, including the vinca alkaloids, taxanes, antibiotics, anthracyclines, DNA alkylators, other DNA damaging agents, hormones, and interferons. More potent analogs of existing drugs and novel agents directed at new targets are continuously being developed. Over the last few years, agents that affect COX-2, PPARγ, and various signal transduction pathways have received much attention. To identify which agents are effective for which types of tumors, it is important to develop accurate in vitro and preclinical in vivo screening systems that can identify the cytotoxic and/or cytostatic potential of an agent on established tumor cell lines or cells isolated from individual fresh cancer biopsy specimens removed from cancer patients. Chemosensitivity testing allows the selection of drugs that appear sensitive in the laboratory, thus offering patients a better chance of response.

One of the main problems associated with chemotherapy has been that patient tumors with the same histology do not necessarily respond identically to the same agent or dose schedule of multiple agents. Identifying the presence of resistance mechanisms and other determinants for drug sensitivity in order to classify tumors into response categories has been an ongoing research effort. Advances in our understanding of the genetic and protein fingerprints of primary tumors and their metastases has opened a door to the possibility of customizing therapy to individuals. There is accumulating evidence suggesting that laboratory screening of samples from a patient's tumor may help select the appropriate treatment(s) to administer, thereby avoiding ineffective drugs, and sparing patients the side effects normally associated with these agents.

The aim of these two volumes on *Chemosensitivity* of the *Methods in Molecular Medicine* series, is to comprehensively present protocols that can be used to (a) assess chemosensitivity in vitro and in vivo, and (b) assess parameters that modulate chemosensitivity in individual tumors. Volume I presents an overview in Chapter 1 and then covers *In Vitro Measures of Chemosensitivity*, includes clonogenic, colorimetric, fluorometric, and histochemical approaches. Volume II, Part I, *Measurements of DNA Damage, Cell Death, and Regulators of Cytotoxicity*, includes methods to detect chromosome loss and breakage, changes in cell cycle, expression of members of the bcl-2 family of proteins, expression of caspases and PARP cleavage, metabolic factors influencing sensitivity, measurements of drug retention, expression of drug resistance proteins, and measurements of ceramide and sphingolipids associated with drug sensitivity. Volume

II, Part II, *Genomics, Proteomics, and Chemosensitivity,* addresses DNA microarrays for gene profiling, genetic manipulation to identify genes regulating chemosensitivity, proteomics using 2D-PAGE and mass spectrometry, and bioinformatics approaches. The last part, *In Vivo Animal Modeling of Chemosensitivity,* covers protocols to establish clinically meaningful metastatic and orthotropic models of solid and liquid tumors, statistical approaches to analyze preclinical data, and animal imaging approaches that can be used to assess chemosensitivity such as GFP-tagged genes, SPECT using ^{99m}Tc-annexin, PET imaging with ^{18}FDG, and magnetic resonance imaging.

Each chapter is written by someone experienced with the methodology and contains a detailed introductory section with references of how the technique has been used in the past, a list of materials and equipment needed to perform the assay, and a step-by-step set of instructions for each method. At the end of each chapter a "Notes" section is included with useful information, helpful hints, and problems and pitfalls to be aware of, in order to make the assay run smoothly and allow for easy interpretation of data.

Rosalyn D. Blumenthal

Contents

Color Plate

The following illustrations appear in the color plate that follows page 238.

Chapter 24:

Figure 1, p. 364, Molecular basis for Annexin A5 imaging.

Figure 2, p. 365, Molecular structure of human Annexin A5.

Figure 5, p. 373, ^{99m}Tc-Annexin A5 uptake as seen by SPECT and autoradiography.

Figure 6, p. 374, Evaluation of tumor regression post-doxorubicin treatment.

Chapter 26:

Figure 1A, p. 418, Glucose uptake into tumor cells.

Figure 1B, p. 419, ^{18}FDG uptake into tumor cells.

Figure 3B, p. 427, Semiquantitative assessment of ^{18}FDG uptake with the primary cervical tumor.

Contributors

BHARAT AGGARWAL • *Department of Experimental Therapeutics, University of Texas M.D. Anderson Cancer Center, Houston, TX, USA*
LEI BAO • *Department of Molecular Sciences, The University of Tennessee Health Science Center, Memphis, TN, USA*
TARIK Z. BELHOCINE • *Department of Nuclear Medicine, Jules Bordet Cancer Institute, Brussels, Belgium*
GIOVANNI L. BERETTA • *Istituto Nazionale Tumori, Milan, Italy*
SERGIO BERNARDINI • *Laboratorio di Biochimica Clinica, Universita di Roma "Tor Vergata," Roma, Italy*
ALOK C. BHARTI • *Department of Experimental Therapeutics, University of Texas M.D. Anderson Cancer Center, Houston, TX, USA*
FRANCIS G. BLANKENBERG • *Division Pediatric Radiology, Stanford University School of Medicine, Palo Alto, CA, USA*
ROSALYN D. BLUMENTHAL • *Garden State Cancer Center, Belleville, NJ, USA*
JAMES K. BREAUX • *Rebecca and John Moores UCSD Cancer Center, University of California–San Diego, La Jolla, CA, USA*
EMMA DAS-GUPTA • *Academic Haematology, Nottingham City Hospital, Nottingham, UK*
YVES A. DECLERCK • *Division of Hematology-Oncology, Keck School Medicine, University Southern California, Los Angeles, CA, USA*
Q. PING DOU • *Wayne State University School of Medicine, Detroit, MI, USA*
GIORGIO FEDERICI • *Laboratorio di Biochimica Clinica, Universita di Roma "Tor Vergata," Roma, Italy*
MICHAEL FENECH • *CSIRO Health Science and Nutrition, South Australia, Australia*
LAURA GATTI • *Istituto Nazionale Tumori, Milan, Italy*
CICEK GERCEL-TAYLOR • *Department of Obstetrics and Gynecology and Women's Health, University of Louisville, Louisville, KY, USA*
RONALD M. HAMELIK • *Division of Experimental Therapeutics, University of Miami, Miami, FL, USA*
ROBERT M. HOFFMAN • *Department Surgery, University of California–San Diego, and AntiCancer Inc., San Diego, CA, USA*
SEIJI ITO • *Department of Gastroenterological Surgery, Aichi Cancer Center Research Institute, Chikusa-ku, Nagoya, Japan*

GUY JERUSALEM • *Department of Hemtology/Oncology, University Hospital of Liège, Liège, Belgium*
ASLAMUZZAMAN KAZI • *Moffitt Cancer Center & Research Institute, University of South Florida, Tampa, FL, USA*
LEE SU KIM • *Department of Cancer Biology, University of Texas M.D. Anderson Cancer Center, Houston, TX, USA*
YASUHIKO KIYOZUKA • *Department Pathology II, Kansai Medical University, Osaka, Japan*
AWTAR KRISHAN • *Division of Experimental Therapeutics, University of Miami, Miami, FL, USA*
TETSURO KUBOTA • *Department of Surgery, Keio University, Tokyo, Japan*
MICHAEL LAUE • *Institute Anatomy & Cell Biology, University of Saarland, Germany*
NATALIA L. LIEM • *Children's Cancer Institute Australia for Medical Research, South Australia, Sydney, Australia*
RICHARD B. LOCK • *Children's Cancer Institute Australia for Medical Research, South Australia, Sydney, Australia*
GERRIT LOS • *Rebecca and John Moores UCSD Cancer Center, University of California– San Diego, La Jolla, CA, USA*
RICHARD MAZURCHUK • *Roswell Park Cancer Institute, Buffalo, NY, USA*
PEDRO MESTRES-VENTURA • *Institute Anatomy & Cell Biology, University of Saarland, Germany*
REX A. MOATS • *Department of Radiology, Keck School Medicine, University Southern California, Los Angeles, CA, USA*
YOSHINARI MOCHIZUKI • *Department of Gastroenterological Surgery, Aichi Cancer Center Research Institute, Chikusa-ku, Nagoya, Japan*
DAVID E. MODRAK • *Garden State Cancer Center, Belleville, NJ, USA*
ANDRA MOGUET • *Institute Anatomy & Cell Biology, University of Saarland, Germany*
KATHLEEN MURPHY • *Department of Pathology, Johns Hopkins University School of Medicine, Baltimore, MD, USA*
HAYAO NAKANISHI • *Division of Oncological Pathology, Aichi Cancer Center Research Institute, Chikusa-ku, Nagoya, Japan*
MONICA PALLIS • *Academic Haematology, Nottingham City Hospital, Nottingham, UK*
RACHEL A. PAPA • *Children's Cancer Institute Australia for Medical Research, Sydney, Australia*
PAOLA PEREGO • *Istituto Nazionale Tumori, Milan, Italy*
JULIA POLAND • *Institut für Laboratoriumsmedizin und Pathobiochemie, Universitätsklinikum Charite, Berlin, Germany*

JANET E. PRICE • *Department of Cancer Biology, University of Texas M.D. Anderson Cancer Center, Houston, TX, USA*
C. PATRICK REYNOLDS • *USC-CHLA Institute for Pediatric Clinical Research, University of Southern California and Childrens Hospital Los Angeles, Los Angeles, CA, USA*
WERNER SCHMIDT • *Department of Gynecology-Obstetrics, University of Saarland, Germany*
ANETTE SCHOFER • *Institute Anatomy & Cell Biology, University of Saarland, Germany*
NARENDRA P. SINGH • *Department of Bioengineering, University of Washington, Seattle, WA, USA*
PRANAV SINHA • *Institut für Medizinische und Chemische Labordiagnostik, Landeskrankenhaus Klagenfurt, Klagenfurt, Austria*
JOSEPH A. SPERNYAK • *Roswell Park Cancer Institute, Buffalo, NY, USA*
BEE-CHUN SUN • *USC-CHLA Institute for Pediatric Clinical Research, University of Southern California and Childrens Hospital Los Angeles, Los Angeles, CA, USA*
YASUNARI TAKADA • *Department of Experimental Therapeutics, University Texas M.D. Anderson Cancer Center, Houston, TX, USA*
MASAE TATEMUATSU • *Division of Oncological Pathology, Aichi Cancer Center Research Institute, Chikusa-ku, Nagoya, Japan*
ANDREA URBANI • *Zentrale Proteinanalytik, Deutsches Krebsforschungszentrum, Heidelberg, Germany*
SILKE WANDSCHNEIDER • *Zentrale Proteinanalytik, Deutsches Krebsforschungszentrum, Heidelberg, Germany*
ROBERT WIEDER • *University of Medicine & Dentistry of New Jersey, Division Medical Oncology/Hematology, Newark, NJ, USA*
FRANCO ZUNINO • *Istituto Nazionale Tumori, Milan, Italy*

Contents of Volume 1

Index

METHODS IN MOLECULAR MEDICINE™

Series Editor: *John M. Walker*

Chemosensitivity

Volume 2: In Vivo Models, Imaging, and Molecular Regulators

Edited by

Rosalyn D. Blumenthal

Chemosensitivity testing is an ex vivo means of determining or enhancing the cytotoxic and/or cytostatic, or apoptosis-inducing effects of anticancer drugs. In *Chemosensitivity,* leading researchers and physicians working in academia and biotech companies describe their best laboratory methods for assessing chemosensitivity in vitro and in vivo, and for assessing the parameters that modulate chemosensitivity in individual tumors. *Volume 2: In Vivo Models, Imaging, and Molecular Regulators* contains today's best protocols for classifying tumors into response categories and for customizing therapy to individuals. These techniques allow measurements of DNA damage, apoptotic cell death, and the molecular and cellular regulators of cytotoxicity, as well as in vivo animal modeling of chemosensitivity. Highlights include genomic and proteomic approaches to assess chemosensivity, in vivo imaging approaches to assess early response to therapy, and methods to statistically analyze data from in vivo therapy. The protocols follow the successful *Methods in Molecular Medicine*™ series format, each offering step-by-step laboratory instructions, an introduction outlining the principle behind the technique, lists of the necessary equipment and reagents, and tips on troubleshooting and avoiding known pitfalls. The authors also provide guidance on how best to analyze the data derived from the protocols. A companion volume, *Volume 1: In Vitro Assays* contains in vitro and in vivo techniques to identify which new agents or combination of agents are effective for each type of tumor.

Cutting-edge and highly practical, the two volumes of *Chemosensitivity* provide a comprehensive collection of readily reproducible techniques for the in vitro and in vivo screening of new agents and a set of proven approaches to understand mechanistically why certain cancer cell lines (in vitro) of

Features

- **State-of-the-art genomic and proteomic approaches to assess chemosensitivity**
- **Cutting-edge in vivo imaging approaches to assess early response to therapy**
- **Methods to statistically analyze and interpret in vivo therapy data**
- **Measures of cellular and molecular regulators of chemosensitivity**
- **Step-by-step instructions to ensure successful results**
- **Tricks of the trade and notes on troubleshooting and avoiding known pitfalls**

Methods in Molecular Medicine™ • 111
ISSN 1543–1894
Chemosensitivity
Volume 2: In Vivo Models, Imaging, and Molecular Regulators
ISBN: 1-58829-586-9 E-ISBN: 1-59259-889-7

ISBN 1-58829-586-9
9 781588 295866 90000